Published in final edited form as:
*Arthritis Rheum*. 2010 April ; 62(4): 1127–1137. doi:10.1002/art.27312.

# Nonerosive arthritis in lupus is mediated by IFN-α stimulated monocyte differentiation that is nonpermissive of osteoclastogenesis

**Kofi A. Mensah**[1,2], **Alexis Mathian**[3], **Lin Ma**[1], **Lianping Xing**[1], **Christopher T. Ritchlin**[1,4], and **Edward M. Schwarz**[1,5]

[1]Center for Musculoskeletal Research, University of Rochester Medical Center, Rochester, NY, USA

[2]Department of Microbiology and Immunology, University of Rochester School of Medicine and Dentistry, Rochester, NY, USA

[3]Baylor Institute for Immunology Research, Dallas, TX, USA

[4]Allergy, Immunology, Rheumatology Unit, Department of Medicine, University of Rochester Medical Center, Rochester, NY, USA

## Abstract

**Objective—**In contrast to rheumatoid arthritis (RA), Jaccoud arthritis (JA) joint inflammation in systemic lupus erythematosus (SLE) is nonerosive. Although the mechanism responsible is unknown, the anti-osteoclastogenic cytokine interferon-alpha (IFN-α), whose transcriptome is present in SLE monocytes, may be responsible. To test this, we examined effects of IFN-α versus lupus disease on osteoclasts and erosion in the NZBxNZW F1 SLE mouse model with K/BxN serum-induced arthritis (SIA).

**Methods—**Elevated systemic IFN-α levels were obtained by administration of an adenoviral vector expressing IFN-α (Ad-IFN-α). SLE disease was marked by anti-dsDNA antibody titer and proteinuria, and *Ifi202* and *Mx1* expression represented the IFN-α transcriptome. Micro-CT was used to evaluate bone erosions. Flow cytometry for CD11b and CD11c was used to evaluate the frequency of circulating osteoclast precursors (OCP) and myeloid dendritic cells (mDC) in blood.

**Results—**Administration of Ad-IFN-α to NZBxNZW F1 mice induced osteopetrosis. Pre-autoimmune NZBxNZW F1 mice are fully susceptible to focal erosions in the setting of SIA. However, NZBxNZW F1 mice with high anti-dsDNA antibody titers and the IFN-α transcriptome were protected against bone erosions. Ad-IFN-α pre-treatment of NZW mice before K/BxN serum administration also resulted in protection against bone erosion ($r^2$=0.4720, $p<0.01$), which was associated with a decrease in circulating CD11b+CD11c− OCP, and a concomitant increase in CD11b +CD11c+ cells ($r^2$=0.6330, $p<0.05$) that are phenotypic of mDC.

**Conclusion—**These findings suggest that IFN-α in SLE shifts monocyte development toward mDC at the expense of osteoclastogenesis thereby resulting in decreased bone erosion.

### Keywords

Jaccoud arthritis (JA); Lupus; Osteoclast; Interferon-alpha (IFN-α)

5To whom correspondence should be addressed: Dr. Edward M. Schwarz, The Center for Musculoskeletal Research, University of Rochester Medical Center, 601 Elmwood Avenue, Box 665, Rochester, NY 14642, Phone 585-275-3063, FAX 585-756-4727, Edward_Schwarz@URMC.Rochester.edu.

Inflammatory arthritis is one of the most common clinical features in autoimmune disorders (1), and radiologic evidence of joint damage (erosions and joint space narrowing), is observed in almost all patients with rheumatoid arthritis (RA) followed for more than five years (2,3). Pro-inflammatory mediators in RA joints stimulate the production of monocyte/macrophage osteoclast precursors (OCP), which migrate to the bone-pannus interface, and differentiate in response to elevated levels of receptor activator of nuclear factor κB-ligand (RANKL) to become bone-resorbing osteoclasts (OCs) that mediate focal erosions (4–7). Despite the presence of joint deformities on physical examination, not all forms of inflammatory arthritis involve degradation of cartilage and bone resorption. For example, patients with systemic lupus erythematosus (SLE) often complain of musculoskeletal symptoms, with 50% of patients reporting articular pain on presentation (8,9). Additionally, these patients often develop RA-like deformities (ulnar deviation, tendonopathies and subluxation), but only 4–6% of patients display erosive changes on plain radiographs, and histological assessment of their joint tissue shows mild to moderate synovial hyperplasia, microvascular changes and perivascular inflammation with mononuclear cellular infiltrate (10,11). The joint disease in these SLE patients, commonly referred to as Jaccoud arthritis (JA), is characterized by an absence of radiographic erosive changes, and has a relatively benign prognosis (12). Thus, elucidating the mechanism of non-erosive arthritis in JA could have significant implications for the unmet needs of individuals that suffer from destructive RA.

Interferon-alpha (IFN-α) has emerged as the dominant cytokine that is dysregulated in SLE. IFN-α is mainly expressed by plasmacytoid dendritic cells (pDC), and simulates the differentiation and activation of myeloid dendritic cells (mDC) to present autoantigens (13, 14). Increased serum IFN-α correlates with both lupus disease activity and severity (15–17), and PBMC isolated from these patients express a unique gene expression pattern known as the IFN-α transcriptome (18,19). Intriguingly, this transcriptome reverts to a pattern similar to that expressed in healthy controls following effective steroid therapy (18), which simultaneously causes glucocorticoid-induced osteoporosis (20), thus explaining why this non-erosive SLE phenotype in many patients is broadly overlooked.

Convincing preclinical evidence for an IFN-α model of autoimmunity has also been generated using the New Zealand black (NZB)×New Zealand white (NZW) F1 mouse model of lupus (21,22). These mice develop severe immune complex-mediated glomerulonephritis associated with high serum levels of antinuclear autoantibodies evident at 5 months of age. Moreover, IFNAR1$^{-/-}$ mice have severe osteopenia due to increased circulating OCP and uncontrolled bone resorption (23). Interestingly, the genetic component of the NZB lupus-susceptibility locus on distal chromosome 1 is known to contain the interferon-inducible gene *Ifi202* (24), the up-regulation of which is correlated with disease in these mice and is now used as a surrogate reporter of the IFN-α gene expression profile.

We reasoned that the increased mDC differentiation seen in human SLE and NZBxNZW F1 mice must occur at the expense of osteoclastogenesis, as these cells are derived from the same myelomonocyte precursor (25). Based on this information, we proposed an IFN-α-biased myelopoiesis model to explain the non-erosive nature of JA. In this model, concomitant inflammatory arthritis and lupus stimulate the production and release of myelomonocyte precursors from the bone marrow, which are irreversibly committed toward CD11b+CD11c+ mDC differentiation. Furthermore, we postulated that the mDC precursors have lost all osteoclastogenic potential as a direct result of exposure to elevated systemic IFN-α (25). As such, these cells fail to respond to RANKL in inflamed joints, and focal erosion becomes impossible due to the lack of mature OCs. Here we directly test this hypothesis with serum-induced arthritis (SIA) experiments in NZBxNZW F1 mice, and by injecting Ad-IFN-α into NZW non-SLE mice followed by administration of arthritogenic K/BxN serum. The results

demonstrate that IFN-α is sufficient to induce the non-erosive phenotype observed in JA by prevention of osteoclastogenesis due to myeloid differentiation towards mDC.

## MATERIALS AND METHODS

### Animals, Serum Induced Arthritis, and Ad-IFN-α treatments

NZBxNZW F1 and NZW/LacJ mice were obtained from Jackson Laboratories (Bar Harbor, ME). Experiments were performed on 2-, 5-, and 9-month- old female NZBxNZW F1 mice, and age-matched NZW/LacJ controls. Arthritogenic serum was derived from K/BxN mice and assessed for SIA by intraperitoneal (IP) injection of Balb/c mice (Jackson Laboratories), which are a highly susceptible strain for SIA. Serum was administered by IP injection at a dose of 250 μL per mouse. The recombinant adenovirus vector containing the mIFN-α subtype 5 cDNA (Ad-IFN-α) was propagated as previously described (22). IFN-α expression from the Ad-IFN-α vector was assessed by ELISA on supernatants from 293T cells cultured with the virus compared to uninfected and Ad-Null infected controls. No IFN-α was detected in control cultures, while the supernatant from Ad-IFN-α treated cells expressed 641.5 pg/mL at 24hrs (data not shown). A titer of $10^{11}$ virus particles/mL was retro-orbitally injected into mice 7 days before harvesting organs, blood and limbs for analysis. The mice were handled in accordance with protocols approved by the Institutional Animal Care and Use Committee of the University of Rochester (Rochester, NY, USA).

### Ex vivo osteoclastogenesis

All organs were harvested using aseptic technique. Splenocytes were obtained by homogenizing the spleen over a cell-strainer into 1x PBS. Red blood cells (RBCs) in the collected suspension were lysed with ammonium chloride solution (Stem Cell Technologies, Vancouver, BC, Canada), and the collected cells were cultured in alpha-MEM supplemented with 10% fetal calf serum, 5% penicillin / streptomycin, and 5% nonessential amino acids (Invitrogen, Carlsbad, CA, USA) with a final pH of 7.4. To generate OCs, 10 ng/mL of M-CSF (Cell Sciences, Canton, MA, USA) and 5 ng/mL of RANKL (Cell Sciences) were added to the cells for 7 days with fresh media and cytokines added every 2 days. Cells were then fixed and stained for tartrate-resistant acid phosphatase (TRAP) activity (Sigma-Aldrich, St. Louis, MO, USA) to identify OCs (TRAP+ cells with >3 nuclei).

### Histology

Long bones from one leg of each mouse were fixed in 10% phosphate-buffered formalin, decalcified in 10% EDTA solution for two weeks at room temperature with gentle stirring and embedded in paraffin. Histology sections were prepared from three contiguous 3 mm sections 500 mm apart, which were stained with ABH/orange G or for TRAP using the Diagnostics Acid Phosphatase Kit (Sigma, St. Louis, MO, USA). OCs were quantified from TRAP stained sections.

### Antibodies and flow cytometry

Blood was obtained by cardiac puncture and placed in 0.5% EDTA to prevent clotting. Flow cytometry was then performed on PBMC after lysing RBCs. PBMC were stained for 30 min with CD11b-APC clone M1/70 (BD Pharmingen) and CD11c-PE Cy5.5 clone N418 (eBioscience, San Diego, CA, USA) in 1x PBS containing 4% FCS (for flow cytometry) or sterile 1x PBS without FCS (for FACS) after adding anti-CD16/CD32 to block Fc-receptors (BD Pharmingen, San Jose, CA, USA) for 15 min. If cells could not be analyzed by flow cytometry the same day, they were fixed in 1% PFA and analyzed the following day. Flow cytometry was performed using a FacsCalibur (Becton Dickinson). FACS was performed using either a FACS Vantage or a FACS Aria (Becton Dickinson Immunocytometry Systems,

Bedford, MA). Data analysis was done with WinMDI 2.9 software (Scripps Research Institute, La Jolla, CA, USA).

### Micro-CT and histology analyses of trabecular bone and focal erosions

Tibia obtained from our original SLE study in which NZBxNZW F1 and Balb/c mice were untreated, injected with an empty vector (Ad-Null) or Ad-IFN-α (22) were scanned at high resolution (10–12.5 microns) in an Explore Locus SP scanner (GE Healthcare Technologies, London, ON), and the metaphyseal trabecular bone was analyzed by manual segmentation of gray scale slices using the GE Microview software. The bone volume fraction was determined by contouring a ROI in the metaphyseal trabecular region of the tibia excluding cortical bone, and normalizing the volume of the trabecular bone volume in the ROI to the total volume of the ROI as previously described (26). The Structural Model Index (SMI) was quantified as a measure of the morphology of the trabecular bone, where a SMI of 0 signifies that the structure is mostly plate-like (abnormal osteopetrotic), and a value of 3 indicates a mostly rod-like structure (normal trabeculi) from randomly sampled regions (800 μm×800μm×480 μm) of tibial trabecular bone approximately 100 μm distal to the growth plate were quantified. Talus bone volume was quantified via high-resolution *in vivo* micro-CT (VivaCT 40; Scanco, Southeastern, PA, USA) as previously described (27). Briefly, each joint was scanned at an isotropic resolution of 17.5 μm at 55 keV with cone beam mode. The data were reconstructed via Scanco software into Dicom files for analysis. Amira 3.1 software was used to segment and visualize the bones on the micro-CT scans. The talus was specifically labeled using the Segmentation Editor feature. A density threshold >11,000 AU was set as representing bone, and the labels were reconstructed using the SurfaceGen module to visualize the bone. The threshold was kept constant throughout the study. Since the entire talus is scanned, the volume of this bone, as determined from the TissueStatistics module, was used as a quantitative measure of bone erosion. Osteoclasts numbers in the tibial metaphyses were quantified as TRAP+ multinucleated cells as we have previously described (28).

### Anti-dsDNA antibody ELISA and proteinuria measurement

To measure anti-dsDNA antibody titers in the serum of the NZBxNZW F1 and NZW mice in all treatment groups, blood was obtained by cardiac puncture and centrifuged at 10,000 rpm at room temperature for 5 min. The serum was then transferred to a new tube and used with a mouse anti-dsDNA total Ig ELISA kit (Alpha Diagnostic International, San Antonio, TX, USA) according to manufacturer's instructions.

Urine was collected from mice in all treatment groups at time of death. Proteinuria was assessed by dipstick analysis with Chemstrip® 2 GP Urine Test Strips (Roche Diagnostics, Branchburg, NJ, USA) by applying 15 μl of urine to the dipstick and comparing the reading to the scale on the side of the kit as previously described (22). FCS was used as a positive control for protein while distilled water served as a negative control.

### RNA Analysis

Total RNA was extracted from splenocytes using the Qiagen RNeasy mini kit (Qiagen, Valencia, CA, USA) and subsequently reverse-transcribed into cDNA using the iScript cDNA synthesis kit (BioRad, Hercules, CA, USA). To detect *Ifi202* gene expression, triplicate real-time quantitative RT-PCR reactions were performed using the Rotor-Gene 3000 thermal cycler (Corbett Life Science, Sydney, NSW, Australia). SYBR Green I (Applied Biosystems, Foster City, CA, USA) was used for detection of DNA synthesis. The primers used for *Ifi202* were 5'-CAAGCCTCTCCTGGACCTAA -3' (forward) and 5'-CTAGGATGCCACTGCTGTTG-3' (reverse). *Mx1* primers were 5'-CAGAGGTCAGCAGGACATCC-3' (forward) and 5'-TCGCTTGCACTCTGATGACT-3' (reverse). *β-actin* served as the internal house-keeping

gene control (forward primer sequence 5'-AGATGTGGATCAGCAAGCAG-3', reverse primer sequence 5'-GCGCAAGTTAGGTTTTGTCA-3'). The following cycling conditions were used: 95 °C, 10 min followed by 45 cycles of 95 °C, 15 sec; 58 °C (annealing temperature), 60 sec; 72 °C 15 sec.

### Statistical Analysis

Data are presented as means ± standard error of the mean. Student's *t*-test or analysis of variance (ANOVA) were performed with a significance level of $P<0.05$. Linear regression analyses were performed with a minimum confidence level of 95%. Statistics were calculated using either Microsoft Excel 9.0 software (Microsoft, Redmond, WA, USA) or the GraphPad PRISM software package (GraphPad Software, La Jolla, CA, USA).

## RESULTS

### Lupus susceptibility and systemic IFN-α contribute to osteopetrosis in NZBxNZW F1 mice

As a prelude to the arthritis studies, we first investigated the effects of Ad-IFN-α and genetic background on normal bone remodeling via micro-CT, bone histomorphometry, and histology of tibiae from the mice in our previous SLE study, in which NZBxNZW F1 and Balb/c mice were injected with Ad-IFN-α (22). As previously reported, IFN-α was detected only in the serum of mice treated with Ad-IFN-α, and the serum levels were similar in both strains, peaking at ~700 pg/ml on day 3 and plateauing at ~200 pg/ml by day 10. No differences in metaphyseal OC numbers were observed in any of the control groups as assessed by TRAP stained histology (Balb/c untreated 70±8; Balb/c Ad-Null empty vector 73±9; NZBxNZW F1 untreated 73±7; NZBxNZW F1 Ad-Null empty vector 73±9). However, Balb/c mice treated with Ad-IFNα had a significant decrease in the number of metaphyseal OC (26±6; $P<0.01$), which inhibited resorption of the primary spongiosa as evidenced by irregular trabeculi (Figure 1). Thus, demonstrating the direct effects of IFNα on OC numbers *in vivo*. The NZBxNZW F1 background markedly enhanced the Ad-IFN-α effects, as OC numbers were significantly lower than controls and Balb/c mice (4±2; $P<0.05$), and the mice had severe osteopetrosis.

### NZBxNZW F1 mice with signs of lupus and elevated Ifi202 expression are resistant to bone erosions during inflammatory arthritis

To assess the effects of lupus genetics, lupus disease and IFN-α on erosive inflammatory arthritis independently and collectively, we investigated OCP, OC numbers and bone loss in NZBxNZW F1 mice with and without SIA: before the onset of lupus (2-month-old), with established lupus (5-month-old) and with severe lupus (9-month-old). We evaluated age- and gender-matched NZW mice as controls, rather than Balb/c, because they are a parental strain, and used the results from our Ad-IFN-α Balb/c studies as the control to interpret the direct effects of IFN-α alone in WT mice. Moreover, the *Ifi202* gene polymorphism within the Nba2 locus is contributed by the NZB parental strain, and its expression is not detected at elevated levels in the NZW parental strain. It has also been shown that NZW mice congenic for the Nba2 locus develop high anti-nuclear autoantibodies characteristic of SLE (24). Based on this, we used NZW and NZW injected with Ad-IFN-α as negative and positive controls respectively, and utilized *Ifi202* gene expression as a marker of the IFN-α transcriptome in SLE.

First, we confirmed the presence of lupus disease and the IFN-α transcriptome status of these mice by measuring their serum anti-dsDNA antibody titers, urine protein levels, and *Ifi202* expression levels in splenocytes (Figure 2). The results demonstrated the predicted age-dependent disease progression in NZBxNZW F1 mice, and the complete absence of these lupus markers in NZW mice. However, consistent with the congenic Nba2 studies, we found that NZW mice given Ad-IFN-α had serum anti-dsDNA autoantibodies, proteinuria, and *Ifi202* levels that were significantly higher than age- and gender-matched control NZW mice.

Moreover, these markers of lupus were induced to similar levels in NZW mice given Ad-IFN-α irrespective of age, demonstrating a direct effect of this cytokine. In order to test if there is a direct correlation between the IFN-α transcriptome and lupus markers in our mouse model, we performed a linear regression analysis, which showed that increased *Ifi202* gene expression is significantly correlated with increased anti-dsDNA autoantibody titers (Figure 2D). We also evaluated the association between anti-dsDNA autoantibody titers and expression levels of *Mx1*, another IFN-α-inducible gene, to be sure that our observations were representative of other markers of the IFN-α transcriptome and not solely *Ifi202*. Mice with low anti-dsDNA autoantibody titers had low *Mx1* gene expression levels, while those with high anti-dsDNA autoantibody titers and proteinuria had significantly higher *Mx1* gene expression (data not shown).

To study the erosive nature of inflammatory arthritis in the setting of SLE, we used the serum transfer model. In this model, arthritogenic serum from K/BxN mice is transferred to susceptible strains in order to induce arthritis (29). Interestingly, Ji et al. have previously used clinical assessment of ankle swelling to define the NZW, NZBxNZW F1, and NZB strains as susceptible, moderately susceptible and non-susceptible, respectively, to this model of serum induced arthritis (SIA) (30). However, the effects of SIA on bone mass, OCP or OC in these strains has yet to be determined. To test this effect, we performed micro-CT on the ankles of untreated controls and mice with SIA, to determine the degree of arthritic erosions in the talus as we have previously described (27). Figure 3A shows representative 3D micro-CT reconstruction images of the talus from 5-month-old animals. Consistent with prior results on joint inflammation, we found marked bone erosions in NZW + SIA mice, but not in the control NZW and NZBxNZW F1 mice, nor the NZBxNZW F1 + SIA mice. Quantification of the talus bone volume by 3D-CT reconstruction confirmed these significant differences, which were age-dependent in the NZBxNZW F1 mice. Figure 3B shows that at 2 and 5 months, untreated NZBxNZW F1 mice had a higher bone volume compared to gender- and age-matched female NZW mice (1.16±0.02 $mm^3$ vs. 1.07±0.04 $mm^3$) and (1.19±0.07 $mm^3$ vs. 1.04±0.06 $mm^3$). Talar bone volume was similar between NZBxNZW F1 mice and NZW mice aged 9 months (1.08±0.05 $mm^3$ vs. 1.09±0.04 $mm^3$). Significant talar bone loss and erosions were observed on micro-CT at 5 days post-injection with K/BxN serum in NZW mice compared to NZW mice not receiving K/BxN serum at all ages tested (2 mo.: from 1.07±0.04 $mm^3$ to 0.94±0.06 $mm^3$, 5 mo.: from 1.04±0.06 $mm^3$ to 0±0.03 $mm^3$, and 9 mo.: from 1.09±0.04 $mm^3$ to 0.88 ±0.03 $mm^3$). In contrast, NZBxNZW F1 mice showed a significant decrease in talar bone volume after K/BxN serum transfer only at 2 months of age (from 1.16±0.02 $mm^3$ to 0.97±0.10 $mm^3$). Though they did show evidence of slight ankle thickening on gross observation, 5- and 9-month-old NZBxNZW F1 mice injected with K/BxN serum were resistant to erosive inflammatory arthritis (talar bone volume pre- and post-SIA: 1.19±0.07 $mm^3$ vs. 1.18±0.07 $mm^3$ and 1.08±0.05 $mm^3$ vs. 1.13±0.13 $mm^3$ respectively).

To demonstrate the direct effects of strain and systemic IFN-α on OC in this model, we analyzed histology from the ankle and knee joints of these mice (Figure 3C). The results showed that NZBxNZW F1 mice treated with K/BxN serum had less inflammatory infiltrate in juxtaarticular regions compared to NZW mice with SIA, where inflammatory infiltrate is prominent. Moreover, TRAP staining showed increased numbers of OC in the juxtaarticular region of NZW mice with SIA, but not in this region in NZBxNZW F1 mice. Histomorphometric quantification confirmed the significant decrease in OC numbers in NZBxNZW F1 versus NZW mice at all time points (Figure 3D - left). However, when we evaluated the circulating OCP frequency in these mice via *ex vivo* formation of TRAP+ MNC from splenocyte cultures, we found the significant decrease in NZBxNZW F1 to be age-dependent (Figure 3D - right), similar to the age dependent presentation of lupus markers (Figure 2).

### NZBxNZW F1 lupus mice and NZW mice given Ad-IFN-α have a decrease in CD11b+CD11c− OCP and an increase in CD11b+CD11c+ mDC precursors in their PBMC

In addition to seeing a decrease in the number of OC in NZBxNZW F1 mice in the setting of SIA, we also observed that the OC arising from NZBxNZW F1 with SIA were significantly smaller than those from NZW with SIA (Figure 4A). Furthermore, very few OC were observed from *ex vivo* osteoclastogenesis from splenocytes cultured from NZW mice given Ad-IFN-α in the setting of SIA (Figure 4A). These data in conjunction with the data in Figure 3 suggest that the major inhibitory effects of IFN-α and lupus on focal erosions are exerted on the circulating OCP population. OC derive from a monocytic precursor that can also give rise to macrophages and mDC under the appropriate cytokine stimulation (31). As IFN-α has been shown to drive monocyte precursor development towards mDC differentiation in SLE (32), we hypothesized that the decreased osteoclastogenesis observed in the NZBxNZW F1 and NZW mice given Ad-IFN-α was a result of biased circulating monocyte differentiation away from OC and toward mDC. Since cell-surface co-expression of CD11b and CD11c is a known immunophenotype of mDC in PBMC (33), we tested our hypothesis by measuring the percentage of CD11b+CD11c+ versus CD11b+CD11c− PBMC in the mice. The results showed that 9-month-old NZBxNZW F1 mice with SLE-like disease had a higher proportion of CD11b+CD11c+ PBMC relative to age- and gender-matched NZW mice (Figure 4B). Moreover, the 7-fold increase in CD11b+CD11c− PBMC observed in NZW mice with SIA, was completely absent in NZBxNZW F1 mice with non-erosive SIA (Figure 4C). Furthermore, NZW mice with SIA and Ad-IFN-α only had a 3-fold decrease in CD11b+CD11c- PBMC, with a concomitant 5-fold increase in CD11b+CD11c+ PBMC, compared to NZW + SIA controls (Figure 4D). These data confirm the *ex vivo* osteoclastogenesis results (Figure 3D & 4A), and demonstrate the dramatic effects of IFN-α on circulating monocyte populations.

### Presence of an elevated IFN-α transcriptome correlates significantly with a greater CD11b +CD11c+ population and decreased bone loss from erosions in inflammatory arthritis

We performed linear regression analyses comparing *Ifi202* gene expression levels, talar bone volume and the percentages of CD11b+CD11c− and CD11b+CD11c+ PBMC in the mice we studied. First, we found a statistically significant inverse correlation between circulating OCP versus mDCP (Figure 5A). Next, we found that higher talar bone volume correlated significantly with a greater percentage of CD11b+CD11c+ PBMC (Figure 5B). We also found that there was a statistically significant positive correlation between *Ifi202* gene expression and both the percentage of CD11b+CD11c+ PBMC and talar bone volume (Figure 5C and 5D). Similarly, higher average talar bone volume was observed among mice with high *Mx1* expression levels (Figure 5E). Thus, although the molecular mechanisms for these associations remain to be elucidated, the results presented here provide the first direct evidence that the IFN-α transcriptome induced during lupus dominantly shifts myeloid differentiation towards mDC in a manner that is non-permissive for osteoclastogenesis and focal erosion.

## DISCUSSION

It is established that the common myelomonocyte progenitor cell can differentiate into CD11b +CD11c+ mDC or CD11b+CD11c− OCP depending on the cytokine milieu. Previous research demonstrated that elevated levels of IFN-α influence myelomonocyte development into mDC, and that mDC are a major cellular mediator of SLE pathology (13). It has also been shown that inflammatory erosive arthritis can be marked by an elevation in the CD11b+CD11c− population. While it is known that JA is typically non-erosive, and that IFN-α is considered the dysregulated cytokine in SLE, knowledge of a potential link between these two factors and myelopoiesis is scarce. Using the SIA model in conjunction with the NZBxNZW F1 model, we were able to add to the existing literature on SLE, myelopoiesis, and bone, by studying the

effect of SLE disease and the effect of IFN-α in particular on the development of bone erosion in inflammatory arthritis.

The current etiologic model for the role of dysregulated IFN-α in SLE suggests that pathologically elevated levels of IFN-α are released from pDC after stimulation by an unknown factor (13). Though early evidence of this came from detection of elevated serum levels of IFN-α, ELISA for IFN-α has been reported not to be very sensitive or reliable for measuring naturally elevated IFN-α levels because the range of detection antibodies would need to account for the approximately 14 known IFN-α isoforms. A more widely accepted method of determining IFN-α levels in SLE is to measure the levels of IFN-α-inducible genes since all IFN-α isoforms bind the same receptor and induce the same signaling cascade leading to gene expression (34). Though many IFN-α-inducible genes have been identified as correlating with SLE pathophysiology, the *Ifi202* gene has been best characterized as a susceptibility gene in the NZBxNZW F1 model we used in this study (24). In NZB mice, natural levels of serum IFN-α were undetectable by ELISA, and CpG ODN injection was needed to see significant serum IFN-α levels detectable by ELISA compared to Balb/c controls (35). Despite this, NZB mice have elevated expression of *Ifi202* compared to Balb/c and C57Bl/6 mice (24). The NZBxNZW F1 mice in our study exhibited elevated levels of *Ifi202* mRNA expression compared to NZW controls at all ages. This is in accordance with previous literature that showed this gene not to be elevated in NZW mice (24). Interestingly, the *Ifi202* gene expression level was elevated even at 2 months of age though anti-dsDNA antibodies and proteinuria were not significantly different at this age from that seen in NZW mice. This may be explained by a gradual skewing of the monocyte differentiation program toward mDC with the age-related accumulation of IFN-α, and increasing numbers of circulating mDC presenting autoantigens, thereby breaking self-tolerance over time. Additionally, variables such as estrogen status and environmental factors likely contribute to the timing of autoantibody formation which precedes disease onset. Nevertheless, in these pre-autoimmune mice, induction of systemically elevated IFN-α via injection of Ad-IFN-α resulted in SLE disease features suggesting that innate barriers to a break in tolerance can be overcome if these mice exceed threshold levels of IFN-α.

As seen in human disease, the presence of SLE protected NZBxNZW F1 mice from developing bone erosions in the setting of inflammatory arthritis. When these mice were at an age where they did not exhibit SLE disease features (anti-dsDNA autoantibodies or proteinuria), they displayed a similar susceptible to SIA bone erosions as the non-SLE NZW mice were at all ages. To explain this, we examined osteoclastogenesis in these animals. We observed that NZBxNZW F1 mice had lower numbers of OC *in vivo* at the site of resorption compared to NZW mice. This could be the result of decreased circulating OCP, and/or expression of local factors at the site of resorption that inhibit osteoclastogenesis in mice with SLE-like disease. To address this, we also examined the *ex vivo* osteoclastogenic potential of circulating OCP from NZBxNZW F1 mice. Our results show that although SIA is capable of inducing osteoclastogenesis in both NZW and NZBxNZW F1 strains, it is more effective in mice without SLE. These data demonstrate that the reduced degree of bone erosion seen in inflammatory arthritis in NZBxNZW F1 mice is the result of a more global anti-osteoclastogenic process and not solely a local effect. Furthermore, our finding that NZBxNZW F1 mice with SLE-like disease had a greater percentage of circulating mDCP compared to the percentage of circulating OCP supports the idea that the global deficit in osteoclastogenesis seen in these mice is from a skewing of myelomonocytic differentiation.

The osteoclastogenesis, bone erosion, and mDCP frequency findings in the NZBxNZW F1 mice could be explained by events associated with SLE, or could represent another direct effect of IFN-α in SLE pathophysiology. The injection of Ad-IFN-α induced *Ifi202* gene expression and the development of SLE disease markers in the NZW mice whereas Ad-Null and uninjected mice did not show these findings. Our results show that the presence of elevated IFN-α levels

was able to mitigate the erosive nature of inflammatory arthritis by globally reducing the number of OC. These findings were explained by an elevation in the relative proportion of mDCP to OCP in the blood. Thus, the artificial induction of elevated systemic IFN-α is capable of replicating the findings we saw in NZBxNZW F1 mice with naturally high levels of IFN-α-inducible *Ifi202* and SLE disease markers. This supports a direct effect of IFN-α on OCP frequency and bone erosion in inflammatory arthritis rather than general events related to SLE.

It is important to note that most of the research on interactions between SLE disease processes and bone pathology has focused on steroid-induced osteoporosis and avascular necrosis of bone, which are prominent side-effects of effective SLE therapy (20). The mechanisms responsible have largely been attributed to glucocorticoid activation of osteoclastogenesis, direct inhibition of osteoblasts, and prolonged suppression of osteogenesis (36–38). Since glucocorticoid therapy reverses the elevation in the IFN-α transcriptome (18), it consequently mitigates the associated protection against bone erosions we have described here. Thus, the studies on steroid-induced bone loss in SLE patients do not conflict with our findings. However, steroid-independent osteopenia is also known to occur in SLE patients, which is somewhat inconsistent with our mouse models. Thus, the complexities of this disease may have dual inhibitor effects on both osteoclasts that results in decrease erosions, and osteoblasts that results in osteopenia, of which the later warrants further investigation.

Taken together, our findings support a new mechanism for the non-erosive nature of inflammatory JA in SLE. We have shown that a naturally elevated or experimentally induced IFN-α transcriptome directly correlates with protection from bone erosions in inflammatory arthritis as a result of biased myelopoiesis toward mDC and away from OC in a mutually exclusive manner. Further research to uncover how IFN-α influences the molecular interactions that promote this skewed differentiation program will help in identifying therapeutic targets for RA and other inflammatory erosive arthritides.

## Acknowledgments

The authors would like to thank Dr. Jacques Banchereau for providing us with the adenoviral vectors and helpful advice. We also thank Nathaniel Miller and Dr. Hani Awad for technical assistance with the micro-CT; and Krista Scorsone, Ryan Tierney and Dr. Matthew Hilton for technical assistance with the histology. This work was supported by research grants from the National Institutes of Health PHS awards UL1 RR24160, AR/AG48697, AR46545, AR54041 and AR56702. Kofi Mensah is a trainee in the Medical Scientist Training Program, NIH grant #T32 GM07356.

## REFERENCES

1. Firestein GS. Evolving concepts of rheumatoid arthritis. Nature 2003;423(6937):356–361. [PubMed: 12748655]
2. Kaarela K, Luukkainen R, Koskimies S. How often is seropositive rheumatoid arthritis an erosive disease? A 17-year followup study. J Rheumatol 1993;20(10):1670–1673. [PubMed: 8295177]
3. Kaarela K, Sarna S. Correlations between clinical facets of outcome in rheumatoid arthritis. Clin Exp Rheumatol 1993;11(6):643–644. [PubMed: 8299257]
4. Kong YY, Feige U, Sarosi I, Bolon B, Tafuri A, Morony S, et al. Activated T cells regulate bone loss and joint destruction in adjuvant arthritis through osteoprotegerin ligand. Nature 1999;402(6759):304–309. [PubMed: 10580503]
5. Gravallese EM, Goldring SR. Cellular mechanisms and the role of cytokines in bone erosions in rheumatoid arthritis. Arthritis Rheum 2000;43(10):2143–2151. [PubMed: 11037873]
6. Ritchlin CT, Haas-Smith SA, Li P, Hicks DG, Schwarz EM. Mechanisms of TNF-alpha- and RANKL-mediated osteoclastogenesis and bone resorption in psoriatic arthritis. J Clin Invest 2003;111(6):821–831. [PubMed: 12639988]

7. Redlich K, Hayer S, Maier A, Dunstan CR, Tohidast-Akrad M, Lang S, et al. Tumor necrosis factor alpha-mediated joint destruction is inhibited by targeting osteoclasts with osteoprotegerin. Arthritis Rheum 2002;46(3):785–792. [PubMed: 11920416]
8. Kaposi M. New reports on knowledge of systemic lupus erythematosus. Arch Dermat u Syph 1872;4:36–78.
9. Stevens, M. The clinical management of systemic lupus erythematosus. Shur, PH., editor. New York: Grune & Stratton; 1983. p. 63-84.
10. Esdaile JM, Danoff D, Rosenthall L, Gutkowski A. Deforming arthritis in systemic lupus erythematosus. Ann Rheum Dis 1981;40(2):124–126. [PubMed: 7224685]
11. Grigor R, Edmonds J, Lewkonia R, Bresnihan B, Hughes GR. Systemic lupus erythematosus. A prospective analysis. Ann Rheum Dis 1978;37(2):121–128. [PubMed: 646463]
12. Molina JF, Citera G, Rosler D, Cuellar ML, Molina J, Felipe O, et al. Coexistence of human immunodeficiency virus infection and systemic lupus erythematosus. J Rheumatol 1995;22(2):347–350. [PubMed: 7738963]
13. Pascual V, Banchereau J, Palucka AK. The central role of dendritic cells and interferon-alpha in SLE. Curr Opin Rheumatol 2003;15(5):548–556. [PubMed: 12960479]
14. Banchereau J, Pascual V, Palucka AK. Autoimmunity through cytokine-induced dendritic cell activation. Immunity 2004;20(5):539–550. [PubMed: 15142523]
15. Hooks JJ, Moutsopoulos HM, Geis SA, Stahl NI, Decker JL, Notkins AL. Immune interferon in the circulation of patients with autoimmune disease. N Engl J Med 1979;301(1):5–8. [PubMed: 449915]
16. Preble OT, Black RJ, Friedman RM, Klippel JH, Vilcek J. Systemic lupus erythematosus: presence in human serum of an unusual acid-labile leukocyte interferon. Science 1982;216(4544):429–431. [PubMed: 6176024]
17. Ytterberg SR, Schnitzer TJ. Serum interferon levels in patients with systemic lupus erythematosus. Arthritis Rheum 1982;25(4):401–406. [PubMed: 6176248]
18. Bennett L, Palucka AK, Arce E, Cantrell V, Borvak J, Banchereau J, et al. Interferon and granulopoiesis signatures in systemic lupus erythematosus blood. J Exp Med 2003;197(6):711–723. [PubMed: 12642603]
19. Baechler EC, Batliwalla FM, Karypis G, Gaffney PM, Ortmann WA, Espe KJ, et al. Interferon-inducible gene expression signature in peripheral blood cells of patients with severe lupus. Proc Natl Acad Sci U S A 2003;100(5):2610–2615. [PubMed: 12604793]
20. Cunnane G, Lane NE. Steroid-induced osteoporosis in systemic lupus erythematosus. Rheum Dis Clin North Am 2000;26(2):311–329. vi–vii. [PubMed: 10768214]
21. Santiago-Raber ML, Baccala R, Haraldsson KM, Choubey D, Stewart TA, Kono DH, et al. Type-I interferon receptor deficiency reduces lupus-like disease in NZB mice. J Exp Med 2003;197(6):777–788. [PubMed: 12642605]
22. Mathian A, Weinberg A, Gallegos M, Banchereau J, Koutouzov S. IFN-alpha induces early lethal lupus in preautoimmune (New Zealand Black x New Zealand White) F1 but not in BALB/c mice. J Immunol 2005;174(5):2499–2506. [PubMed: 15728455]
23. Takayanagi H, Kim S, Matsuo K, Suzuki H, Suzuki T, Sato K, et al. RANKL maintains bone homeostasis through c-Fos-dependent induction of interferon-beta. Nature 2002;416(6882):744–749. [PubMed: 11961557]
24. Rozzo SJ, Allard JD, Choubey D, Vyse TJ, Izui S, Peltz G, et al. Evidence for an interferon-inducible gene, Ifi202, in the susceptibility to systemic lupus. Immunity 2001;15(3):435–443. [PubMed: 11567633]
25. Schwarz EM, Looney RJ, Drissi MH, O'Keefe RJ, Boyce BF, Xing L, et al. Autoimmunity and bone. Ann N Y Acad Sci 2006;1068:275–283. [PubMed: 16831928]
26. Buie HR, Moore CP, Boyd SK. Postpubertal architectural developmental patterns differ between the L3 vertebra and proximal tibia in three inbred strains of mice. J Bone Miner Res 2008;23(12):2048–2059. [PubMed: 18684086]
27. Proulx ST, Kwok E, You Z, Papuga MO, Beck CA, Shealy DJ, et al. Longitudinal assessment of synovial, lymph node, and bone volumes in inflammatory arthritis in mice by in vivo magnetic resonance imaging and microfocal computed tomography. Arthritis Rheum 2007;56(12):4024–4037. [PubMed: 18050199]

28. Flick LM, Weaver JM, Ulrich-Vinther M, Abuzzahab F, Zhang X, Dougall WC, et al. Effects of receptor activator of NFkappaB (RANK) signaling blockade on fracture healing. J Orthop Res 2003;21(4):676–684. [PubMed: 12798068]
29. Matsumoto I, Maccioni M, Lee DM, Maurice M, Simmons B, Brenner M, et al. How antibodies to a ubiquitous cytoplasmic enzyme may provoke joint-specific autoimmune disease. Nat Immunol 2002;3(4):360–365. [PubMed: 11896391]
30. Ji H, Gauguier D, Ohmura K, Gonzalez A, Duchatelle V, Danoy P, et al. Genetic influences on the end-stage effector phase of arthritis. J Exp Med 2001;194(3):321–330. [PubMed: 11489951]
31. Miyamoto T, Ohneda O, Arai F, Iwamoto K, Okada S, Takagi K, et al. Bifurcation of osteoclasts and dendritic cells from common progenitors. Blood 2001;98(8):2544–2554. [PubMed: 11588053]
32. Santini SM, Lapenta C, Logozzi M, Parlato S, Spada M, Di Pucchio T, et al. Type I interferon as a powerful adjuvant for monocyte-derived dendritic cell development and activity in vitro and in Hu-PBL-SCID mice. J Exp Med 2000;191(10):1777–1788. [PubMed: 10811870]
33. Adachi Y, Taketani S, Toki J, Ikebukuro K, Sugiura K, Oyaizu H, et al. Marked increase in number of dendritic cells in autoimmune-prone (NZW x BXSB)F1 mice with age. Stem Cells 2002;20(1): 61–72. [PubMed: 11796923]
34. Hua J, Kirou K, Lee C, Crow MK. Functional assay of type I interferon in systemic lupus erythematosus plasma and association with anti-RNA binding protein autoantibodies. Arthritis Rheum 2006;54(6):1906–1916. [PubMed: 16736505]
35. Lian ZX, Kikuchi K, Yang GX, Ansari AA, Ikehara S, Gershwin ME. Expansion of bone marrow IFN-alpha-producing dendritic cells in New Zealand Black (NZB) mice: high level expression of TLR9 and secretion of IFN-alpha in NZB bone marrow. J Immunol 2004;173(8):5283–5289. [PubMed: 15470074]
36. Ishida Y, Heersche JN. Glucocorticoid-induced osteoporosis: both in vivo and in vitro concentrations of glucocorticoids higher than physiological levels attenuate osteoblast differentiation. J Bone Miner Res 1998;13(12):1822–1826. [PubMed: 9844099]
37. Kim HJ, Zhao H, Kitaura H, Bhattacharyya S, Brewer JA, Muglia LJ, et al. Glucocorticoids suppress bone formation via the osteoclast. J Clin Invest 2006;116(8):2152–2160. [PubMed: 16878176]
38. Yao W, Cheng Z, Pham A, Busse C, Zimmermann EA, Ritchie RO, et al. Glucocorticoid-induced bone loss in mice can be reversed by the actions of parathyroid hormone and risedronate on different pathways for bone formation and mineralization. Arthritis Rheum 2008;58(11):3485–3497. [PubMed: 18975341]

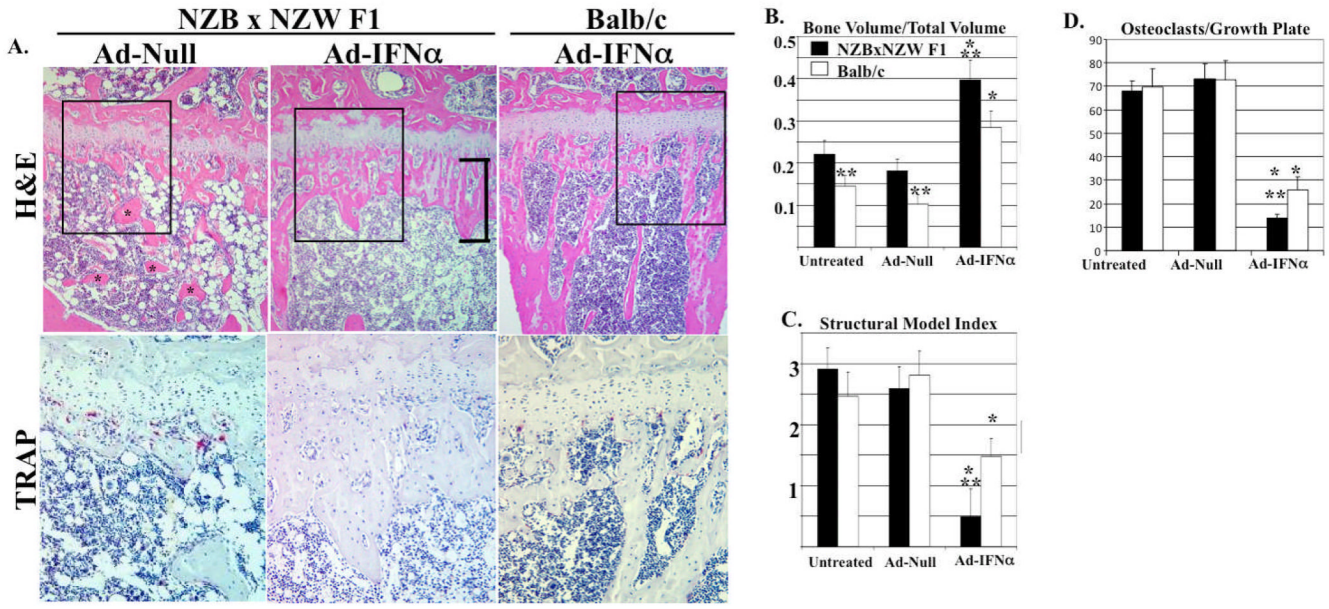


**Figure 1. Systemic IFN-α and NZBxNZW F1 genetic background induce osteopetrosis**

Histology and micro-CT of the tibiae metaphysis from NZBxNZW F1 and Balb/c mice (n=5) untreated, or given $10^{11}$ viral particles of Ad-Null or Ad-IFN-α (22). (A) Representative H&E sections at 10x magnification. Note normal trabeculi (*) in Ad-Null NZBxNZW F1, and their absence in the Ad-IFN-α, which contains an expanded growth plate (bracket). A region of interest (ROI; box in H&E) of a parallel TRAP sections (40x magnification) demonstrating normal numbers in Ad-Null (red cells), and the complete absence of OC (severe osteopetrosis) in Ad-IFN-α NZBxNZW F1 tibia. (B) The bone volume fraction and the (C) Structural Model Index (SMI) were quantified as described in Methods. (D) TRAP+ multinucleated cells (osteoclasts) per growth plate were quantified to confirm osteopetrosis in Ad-IFN-α treated NZBxNZW F1 tibia. The data are presented as the mean ± SEM for each group (* $p<0.05$ vs. untreated and Ad-Null, ** $p<0.05$ vs. Balb/c).

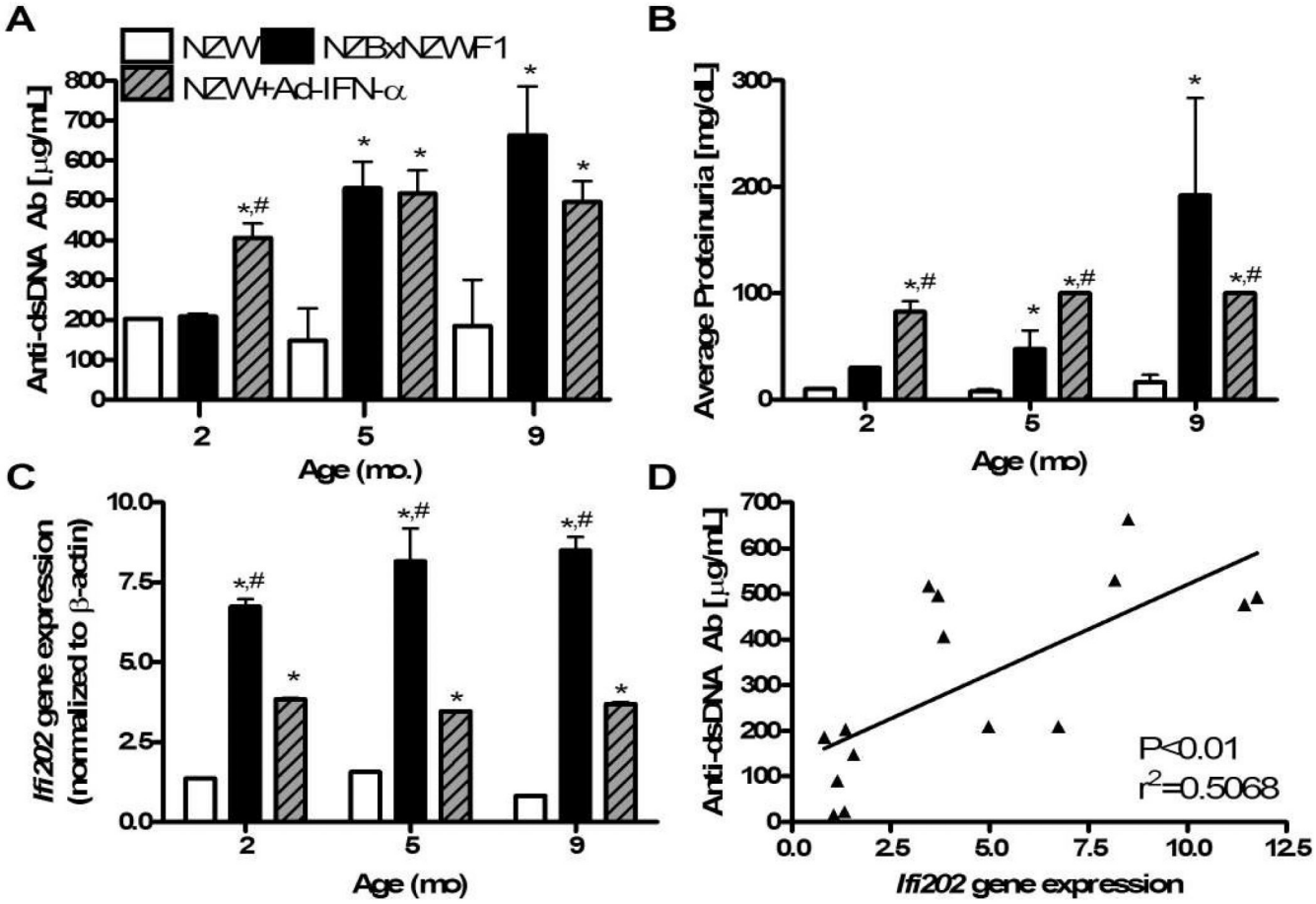


**Figure 2. Lupus disease marker levels and *Ifi202* gene expression correlate in aging NZBxNZW F1 mice and Ad-IFN-α treated NZW mice independent of age**

NZW (white bars), NZBxNZW F1 (black bars), and NZW mice given Ad-IFN-α and SIA (stripped grey bars), were analyzed at the indicated age for: (A) total serum anti-dsDNA autoantibody titers, (B) urine protein levels, and (C) splenocyte *Ifi202* gene expression. The data are presented as the mean ± SEM (n = 3–5 mice per group; * $p<0.05$ versus NZW, ** $p<0.05$ versus NZW + SIA, # $p<0.05$ versus NZBxNZW F1). Serum titers of anti-dsDNA antibodies, proteinuria and *Ifi202* expression data were also obtained for NZW and NZBxNZW F1 mice with SIA, but no differences were found compared to untreated controls (data not shown). (D) Linear regression analysis of the mean anti-dsDNA autoantibody titer versus the mean *Ifi202* gene expression for all 15 groups of mice demonstrates a significant relationship between the lupus markers in these mice.

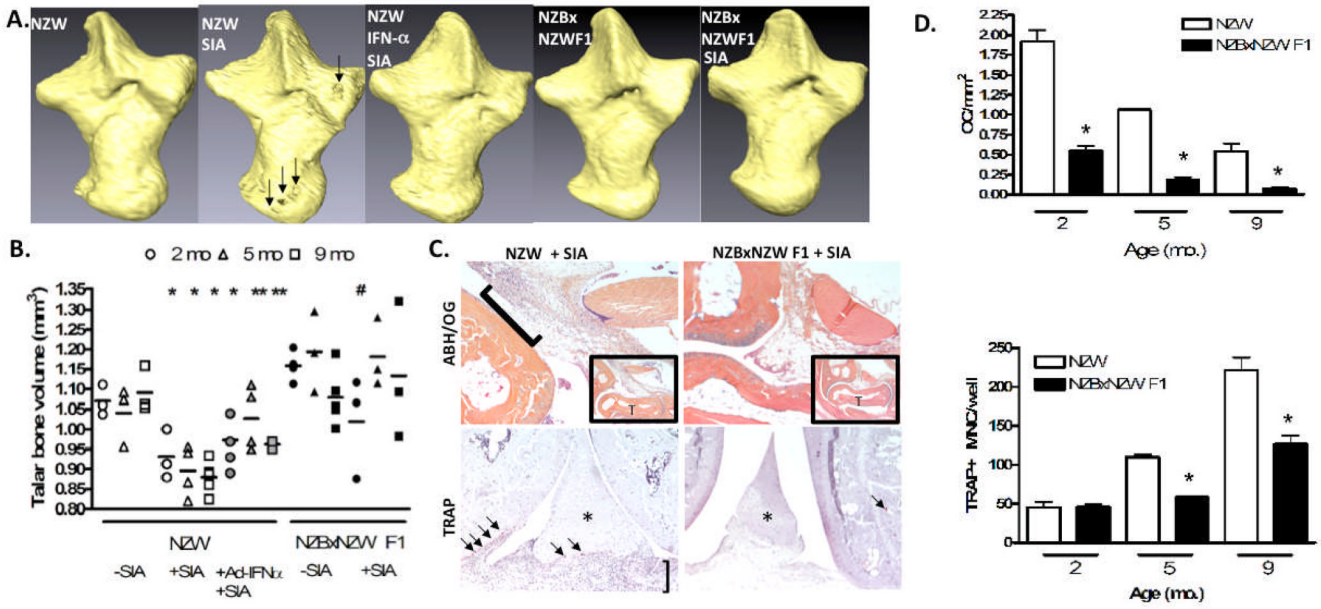


**Figure 3. NZBxNZW F1 mice and Ad-IFN-α treated NZW mice are resistant to arthritis-induced focal erosions and have deceases in OCP and OC**

NZW, NZBxNZW F1, and NZW mice given Ad-IFN-α were untreated or given SIA at the indicated age. (A) Representative reconstructed 3D-CT images of the right taluses are shown to highlight the presence (arrows) or absence of erosions in 5-month-old mice. (B) Individual talar bone volumes of mice (n=the number of symbols) at 2-months (circles), 5-months (triangles), and 9-months (squares) of age, and the mean ± SEM for each group (bar) quantified via 3D-micro-CT (* $p<0.05$ versus NZW, # $p<0.05$ versus NZBxNZW F1). (C) Representative ABH/OG sections at 5x (inset; T=talus) and 10x magnification to highlight SIA-induced inflammation (bracket). Representative TRAP sections of knees at 10x highlight OC (arrows) at the erosion front of the pannus (bracket) in NZW + SIA, while OC could only be found in the growth plate of NZBxNZWF1 + SIA. (D) The number of OC/tibial area (top) and circulating OCP frequency determined by *in vitro* splenocyte osteoclastogenesis (bottom) and are presented as the mean ± SEM for the group (* $p<0.05$ versus NZW).

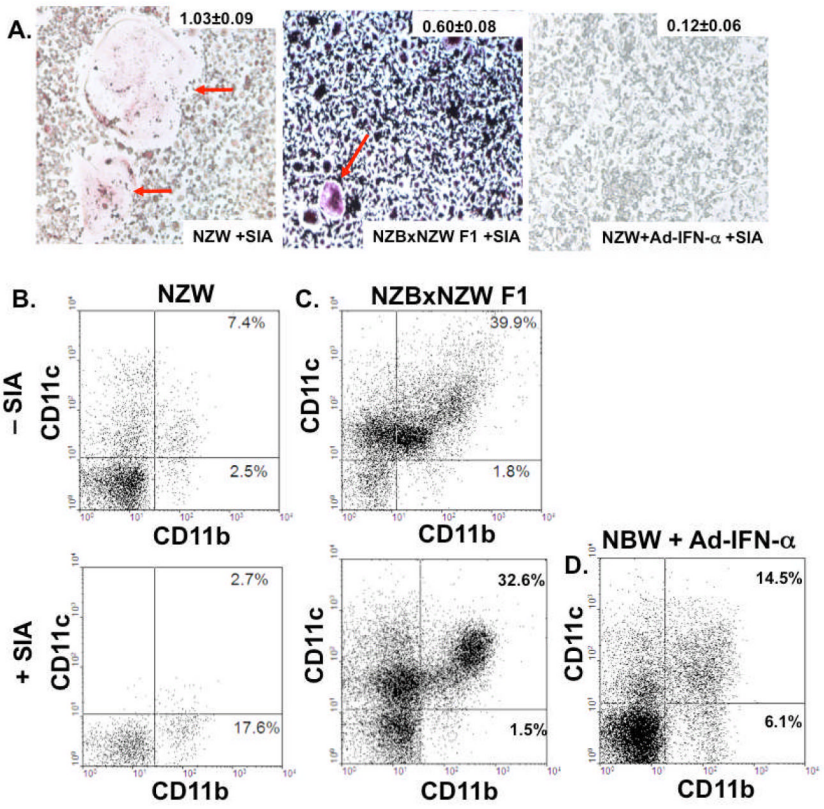


**Figure 4. Non-erosive NZBxNZW F1 mice and Ad-IFN-α treated NZW mice with SIA have a decrease in CD11b+CD11c− OCP and an increase in CD11b+CD11c+ DCP PBMC frequency**

The circulating OCP frequencies in NZW, NZBxNZW F1 and NZW mice given Ad-IFN-α and SIA (n=3 to 5 per group) were determined by *ex vivo* osteoclastogenesis assays performed on splenocytes harvested on day 5. Representative photographs of the TRAP stained cultures (A) are shown to demonstrate the remarkable difference in OC size (indicated by red arrows), which is also presented as mean ± SEM OC area ($mm^2$) for the group. Blood was pooled from 9-month-old NZW (B), NZBxNZW F1 mice (C), and NZW mice treated with Ad-IFN-α and SIA (D), as described in Figure 2, and PBMC were stained with fluorescently labeled antibodies specific for CD11b and CD11c, and analyzed by flow cytometry as described in Methods. Representative dot plots are shown to highlight the percentage of CD11b+CD11c− OCP and CD11b+CD11c+ DCP in the indicated quadrants.

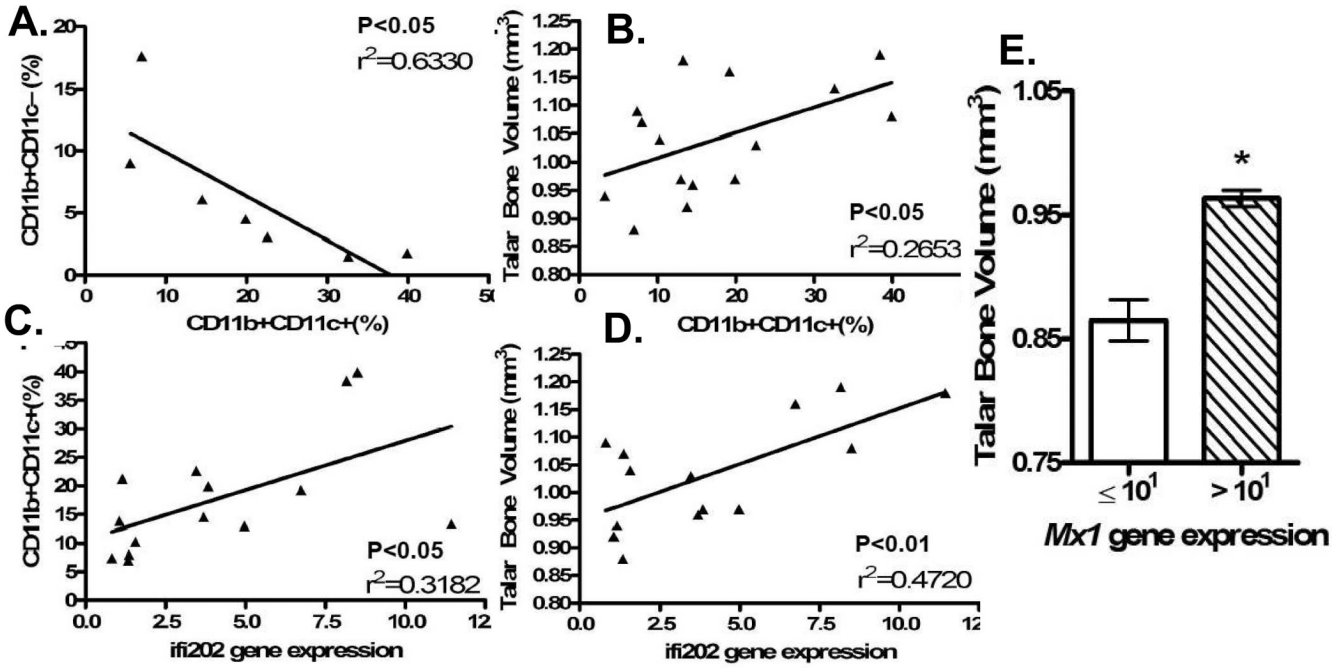


**Figure 5. There is an inverse relationship between OCP and DCP frequency, and a direct correlation between the IFN-α transcriptome in PBMC and bone volume**

To demonstrate that the non-erosive phenotype of inflammatory arthritis during concomitant lupus is mediated by IFN-α stimulated monocyte differentiation that is non-permissive of osteoclastogenesis, we performed linear regression analyses using the flow cytometry, real time RT-PCR, and micro-CT data described in this study. (A) Linear regression analysis of the percentage of CD11b+CD11c− versus CD11b+CD11c+ PBMCs for NZW mice with arthritis and mice with an elevated IFN-α transcriptome. (B) Linear regression analysis of percentage of CD11b+CD11c+ PBMCs and talar bone volume. (C) Linear regression analysis of percentage of CD11b+CD11c+ PBMCs and *Ifi202* gene expression data. (D) Linear regression analysis of talar bone volume and *Ifi202* gene expression data. (E) *Mx1* mRNA levels in PBMC were determined by real time RT-PCR and the samples were divided based on a threshold expression level of $10^1$ and compared to the average talar bone volume of the mice in that group. Individual points and bars represent mean value for 3–5 mice. * $p<0.05$ versus *Mx1* gene expression $<10^1$.